

# Energy Deposition in Polymers

Matthew J. Urffer

## TODO LIST

Expand this section . . . . . 10

# CONTENTS

5			
6	<b>I</b>	<b>Previous Work</b>	<b>6</b>
7	I-A	Spectra Measurements . . . . .	6
8	I-B	Single Collision Energy Loss . . . . .	7
9	<b>II</b>	<b>Introduction to GEANT4</b>	<b>10</b>
10	II-A	Organization of the GEANT4 Toolkit . . . . .	10
11	II-B	GEANT4 Tracking and Secondaries . . . . .	10
12	<b>III</b>	<b>Methods</b>	<b>12</b>
13	III-A	GEANT4 Implementation . . . . .	12
14		III-A1 Detector Geometry . . . . .	12
15		III-A2 Physics Lists . . . . .	14
16		III-A3 Primary Event Generator . . . . .	16
17	III-B	Sensitive Detectors and Hits . . . . .	17
18	III-C	Analysis . . . . .	20
19	III-D	Determination of Energy Deposition . . . . .	21
20	<b>IV</b>	<b>Simulation Validation</b>	<b>24</b>
21	IV-A	Energy Deposition Validation . . . . .	24
22	IV-B	Spectra Validation . . . . .	25
23	<b>V</b>	<b>Results</b>	<b>28</b>
24	V-A	Energy Deposition . . . . .	28
25	V-B	Secondary Electron Energy Distribuion . . . . .	28
26	<b>VI</b>	<b>Conclusions</b>	<b>31</b>
27		<b>References</b>	<b>32</b>

## LIST OF FIGURES

28

29	1	Spectra properties as a function of film thickness . . . . .	6
30	2	Gamma intrinsic efficiency (dashed lines) plotted against neutron counts (solid) . . . . .	7
31	3	Single-collision energy loss spectra for electrons in water [1] . . . . .	8
32	4	Average and median energy transfer in liquid water as functions of incident-electron energy [1] . . . . .	9
33	5	World, Calorimeter, Layer and Absorber and Gap . . . . .	14
34	6	10 Layer Detector with a simulated gamma event . . . . .	15
35	7	Single Collision Energy Loss of Water . . . . .	24
36	8	Gamma Simulation Agreement . . . . .	26
37	9	Neutron Simulation Agreement . . . . .	27
38	10	Simulated Energy Depositon for a Single Film (gammas) . . . . .	29
39	11	Simulated Energy Depositon for a Single Film (neutrons) . . . . .	30
40	12	Simulated kinetic energies of electrons from $^{60}\text{Co}$ interactions . . . . .	30
41	13	Comparison between average neturon and gamma energy deposition . . . . .	31

## LIST OF TABLES

## LISTINGS

43

44	1	Tracking Example . . . . .	11
45	2	World Physical Volume . . . . .	12
46	3	Calorimeter Volume . . . . .	13
47	4	Layer Volume . . . . .	13
48	5	Absorber and Gap Volumes . . . . .	13
49	6	Implemented Physics List . . . . .	15
50	7	Implemented Physics List . . . . .	16
51	8	Primary Event Generator . . . . .	16
52	9	Generate Primaries . . . . .	17
53	10	Calorimeter Hit . . . . .	17
54	11	Sensitive Detector . . . . .	19
55	12	Creating Sensitive Detectors . . . . .	20
56	13	Event Action . . . . .	20
57	14	Run Action . . . . .	21
58	15	Process Hit Collection . . . . .	21
59	16	Run Macro . . . . .	23

## I. PREVIOUS WORK

Previous work on the energy deposition of thin films focused on spectra measurements from fabricated films along with single collision energy loss spectra for physical insights. A sequence of 10%  $^6\text{LiF}$ , 5% PPO-POPOP films in a PS matrix cast to thickness between 15 and 600  $\mu\text{m}$  were fabricated and the response was measured from a gamma source as well as a neutron source. These experiment results are shown in I-A. The single collision energy loss spectra was investigated for electrons in water in order to provide insight on the amount of energy an electron loses in a collision. These results are discussed in Section I-B.

### A. Spectra Measurements

Evidence that the secondary electrons contribute to energy loss can be seen in Figure 1 where there is an increase in the endpoint of the spectra as films become thicker. This increase in the spectra endpoint is indicative of the film producing more light, and as the light collection geometry remained constant, the increase in the endpoint is attributed to a larger energy deposition in the 50  $\mu\text{m}$  film compared to the 15  $\mu\text{m}$  or 25  $\mu\text{m}$  film. Figure 2 shows

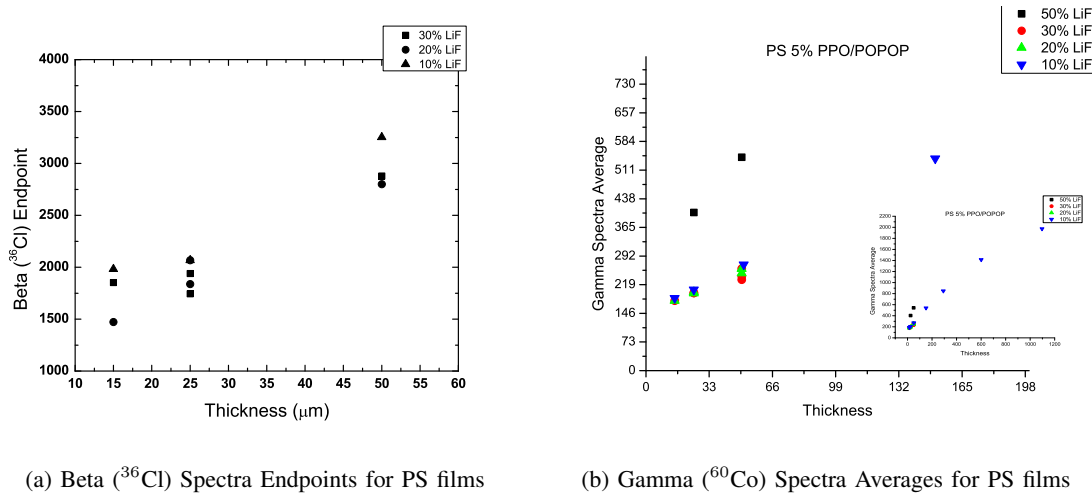


Fig. 1: Spectra properties as a function of film thickness

the intrinsic efficiency of these film from spectra obtained from a  $^{60}\text{Co}$  source. As the film thickness increases the pulse height discriminator at which an intrinsic efficiency of one in a million ( $\epsilon_{int,\gamma} \leq 10^{-6}$ ) is reached also increases. The neutron spectra (shown in the solid lines) does not increase in light yield with increasing thickness, further providing an indication that the thickness of the films can be optimized to maximize the neutron count rates<sup>1</sup> while minimizing the response of the detector to photons.

<sup>1</sup>The neutron count rate is increased with thickness by the increased mass of the detector

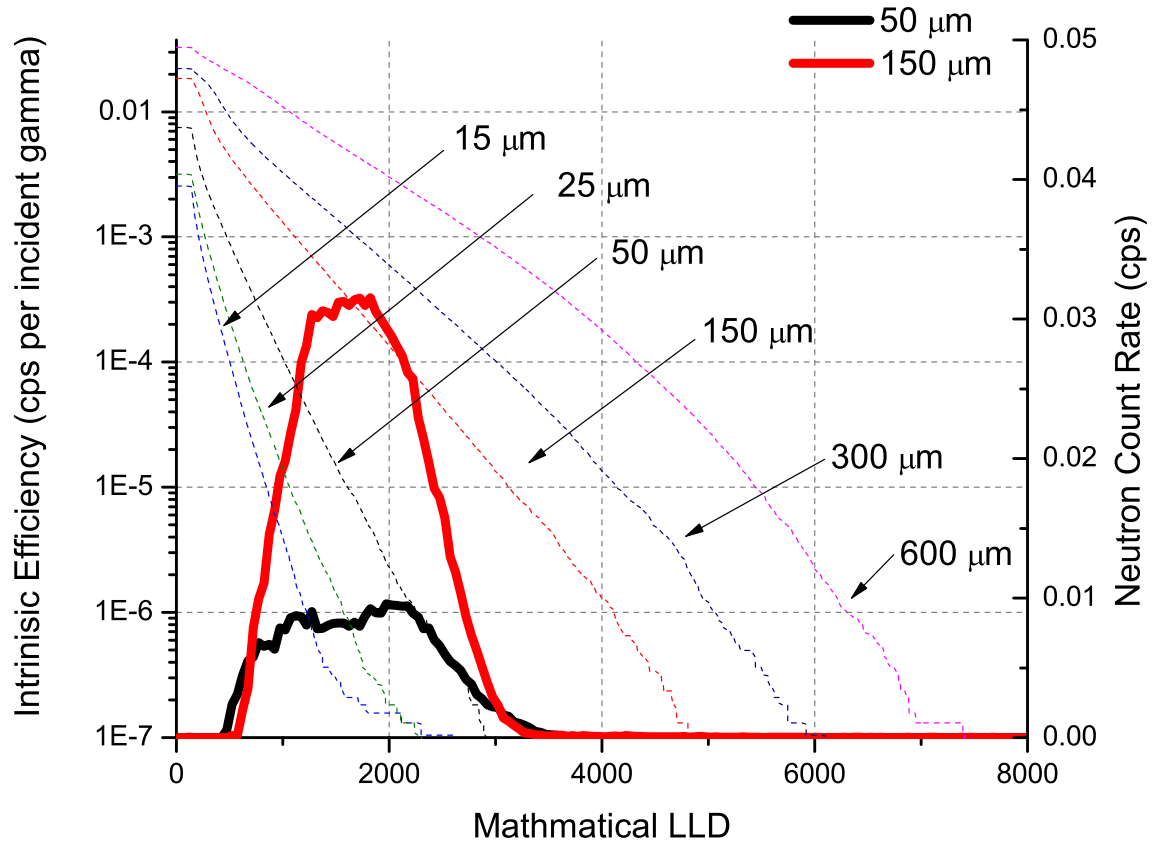


Fig. 2: Gamma intrinsic efficiency (dashed lines) plotted against neutron counts (solid)

### 77 B. Single Collision Energy Loss

78 Single collision energy loss spectra provides the probability that that a given collision will result in an energy loss.  
 79 Provided a spectra of secondary electrons from either the Compton scattered electron or the  $^6\text{Li}$  reaction products it  
 80 is then possible to determine the average energy loss per collision. A single collision energy loss spectra for water  
 81 is shown in Figure 3. For low electron energies ( $< 50$  eV) it is very probable that the electron will lose a majority  
 82 of its energy in a single collision. More energetic electrons, however, tend to lose a lower fraction of there total  
 83 energy. A Compton scattered photon, with an energy in the 100's of keV range, will then lose far less energy per  
 84 collision than an electron in the low keV range liberated from the passage of a neutron reaction product through  
 85 the material. When the average and median energy transfer are plotted as a function of incident electron energy  
 86 (Figure 4) the difference in the energy loss spectra becomes more apparent. For low energies (up to an incident  
 87 electron energy of 100 eV) the average and median energy transfer are roughly equal to each other, about half of  
 88 the incident electron. Past 100 eV average energy increases faster than the median energy transfer implying that

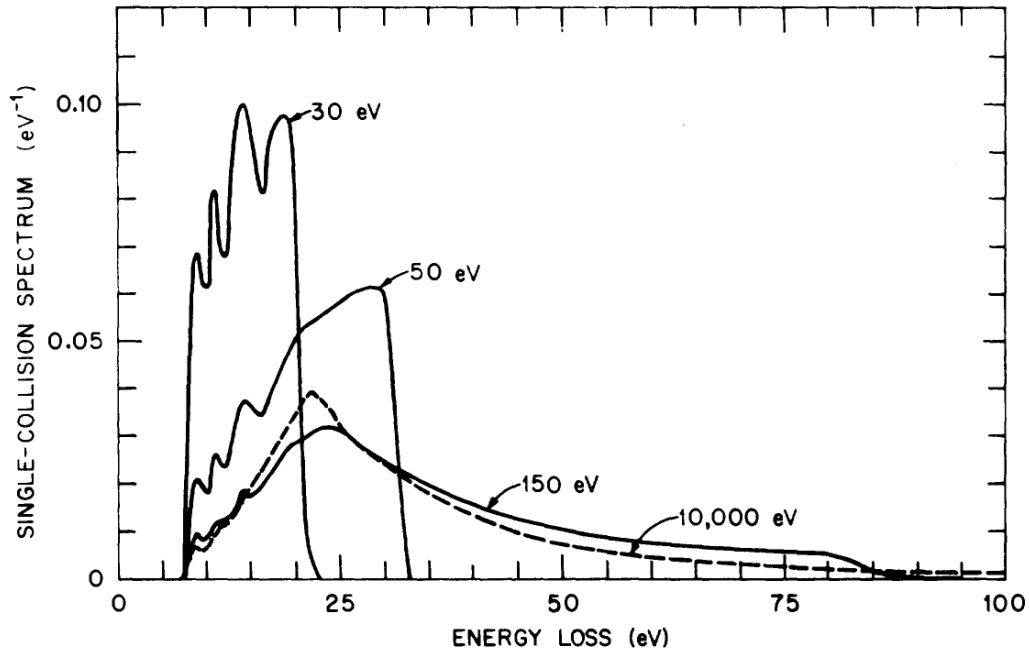


Fig. 3: Single-collision energy loss spectra for electrons in water [1]

89 while a few collisions result in large energy transfers most of the collisions do not. It is also interesting to note that  
 90 the average and median do not increase linearly with the incident energy past 100 eV (the ordinate axis is a log  
 91 scale). In fact, the average energy transferred per collision is mostly bounded by 60 eV even for incident electron  
 92 energies of 10 keV. This is significant because it implies that high energy electrons from photon events will deposit  
 93 a small fraction of their energy in the material.



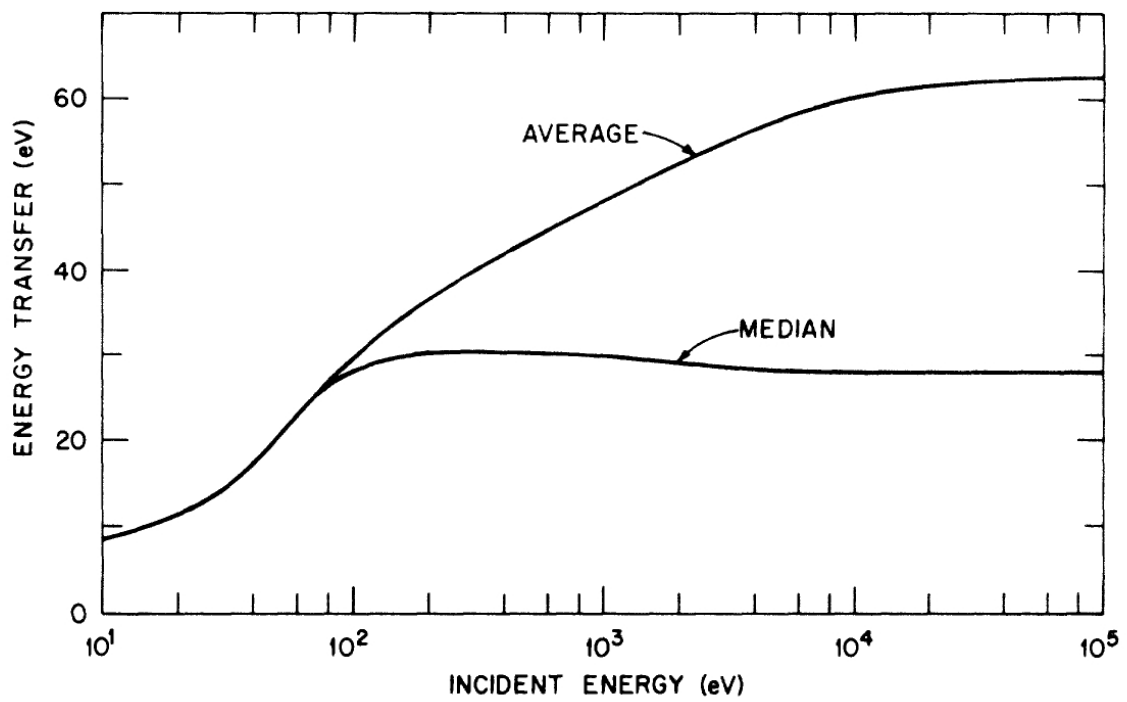


Fig. 4: Average and median energy transfer in liquid water as functions of incident-electron energy [1]

## II. INTRODUCTION TO GEANT4

GEANT4 (GEometry ANd Tracking) is a free, open source, Monte Carlo based physics simulation toolkit developed and maintained at CERN widely used in the physics community [2], [3], [4]. It is based off of the existing FORTRAN based GEANT3, but updated to an object-oriented C++ environment based on an initiative started in 1993. The initiative grew to become an international collaboration of researchers participating in a range of high-energy physics experiments in Europe, Japan, Canada and the United States. As GEANT4 is a toolkit primarily developed for high energy physics, particles are designated according the PDG (Particle Data Group) encoding. In addition, the physics processes are referenced according to the standard model. In the standard model particles are divided into two families, bosons (the force carriers such as photons) and fermions (matter). The fermions consist of both hadrons and leptons. Hadrons are particles composed of quarks which are divided into two classes: baryons (three quarks) and mesons (two quarks). Typical baryons include the neutron and the proton, while an example of a meson is the pion. An example of a lepton is the electron.

### A. Organization of the GEANT4 Toolkit

The GEANT4 toolkit is divided into eight class categories:

- Run and Event - generation of events and secondary particles.
- Tracking and Track - transport of a particle by analyzing the factors limiting the step size and by applying the relevant physics models.
- Geometry and Magnetic Field - the geometrical definition of a detector (including the computation of the distances to solids) as wells as the management of magnetic fields.
- Particle Definition and Matter - definition of particles and matter.
- Hits and Digitization - the creation of hits and their use for digitization in order to model a detector's readout response.
- Visualization - the visualization of a simulation including the solid geometry, trajectories and hits.
- Interface - the interactions between the toolkit and graphical user interfaces and well as external software.

There are then three classes which must be implemented by the user in order use the toolkit. These classes are:

- `G4VUserDetectorConstruction` which defines the geometry of the simulation,
- `G4VUserPhysicsList` which defines the physics of the simulation, and
- `G4VUserPrimaryGeneratorAction` which defines the generation of primary events.

Five additional classes are available for further control over the simulation:

- `G4UserRunAction` which allows for user actions

### B. GEANT4 Tracking and Secondaries

A GEANT4 simulation starts with a run which contains a set number of events. In GEANT4 the Run is the large unit of simulation (represented with a `G4Run` object), which consists of a sequence of events. An event is particular process of interest to the user, such as shooting a single particle at a detector. Typical usage might be to have a run

Expand  
this  
sec-  
tion

firing 1,000 neutrons at a detector, where each neutron is a single event. Each particle transported in GEANT4 is assigned a unique track ID and a parent ID. The particle that initiates the event is given a parent ID of 0 and a track ID of 1. If the parent particle has a collision, and produces a secondary particle, this secondary particle is then given a parent ID of 1 (corresponding to the first secondary) and a track ID of 2. Secondaries are tracked in GEANT4 utilizing a stack in which the most recent secondary (and its cascade) is tracked first.

Listing 1 provides an example from the verbose output of GEANT4 of the tracking. The initial particle in the event is the neutron because it has a parent ID of 0. The alpha and triton are the secondaries produced by this collision. The alpha is assigned a parent ID of 1 (corresponding to the first generation) with a track ID of 3. The triton is also assigned a parent ID of 1, but with a track ID of 2.

Listing 1: Tracking Example

```

137 *****
138 * G4Track Information: Particle = neutron, Track ID = 1, Parent ID = 0
139 *****
140
141
142 Step#  X(mm)  Y(mm)  Z(mm) KinE(MeV)  dE(MeV)  StepLeng  TrackLeng  NextVolume  ProcName
143 0      0      0      -6.59  2.5e-08      0      0      0      Absorber  initStep
144 1      0      0      -3.64      0      0      2.95      2.95      Absorber  NeutronInelastic
145 :----- List of 2ndaries -- #SpawnInStep= 2( Rest= 0, Along= 0, Post= 2), #SpawnTotal= 2 -----
146 :      0      0      -3.64      2.73      triton
147 :      0      0      -3.64      2.05      alpha
148 :----- EndOf2ndaries Info -----
149
150 *****
151 * G4Track Information: Particle = alpha, Track ID = 3, Parent ID = 1
152 *****
153
154 Step#  X(mm)  Y(mm)  Z(mm) KinE(MeV)  dE(MeV)  StepLeng  TrackLeng  NextVolume  ProcName
155 0      0      0      -3.64      2.05      0      0      0      Absorber  initStep
156 1 -0.000201 0.000128  -3.64      2.01  0.0491 0.000266  0.000266  Absorber  ionIoni
157 2 -0.00049 0.000312  -3.64      1.93  0.0705 0.000381  0.000647  Absorber  ionIoni
158
159 *****
160 * G4Track Information: Particle = triton, Track ID = 2, Parent ID = 1
161 *****
162
163 Step#  X(mm)  Y(mm)  Z(mm) KinE(MeV)  dE(MeV)  StepLeng  TrackLeng  NextVolume  ProcName
164 0      0      0      -3.64      2.73      0      0      0      Absorber  initStep
165 1 0.000339 -0.000215  -3.64      2.71  0.0116 0.000447  0.000447  Absorber  hIoni
166

```

### III. METHODS

A discussion of the steps necessary to implement the simulation of energy deposition in GEANT4 follows. This involved writing the code for the simulation, as well as correctly interpreting the output. As such, this section is organized by first examining the process of setting up the simulation and then will go into the analysis of the results from the toolkit.

#### A. GEANT4 Implementation

A large focus of this work was on creating a working simulation of the GEANT4 toolkit. Preliminary attempts were made to install GEANT4 on a Windows based machine linking to Microsoft Visual Studio. While these attempts were successful, a larger scale computing environment was desired. GEANT4 was then installed on the University of Tennessee's nuclear engineering computing cluster, along with the necessary visualization drivers and data files. Brief documentation on compiling simple examples on the cluster are available at the necluster wiki<sup>2</sup>. For convenience a subversion repository was created to manage the developed code base, and all source code is available by anonymous checkout from <http://www.murphs-code-repository.googlecode.com/svn/trunk/layeredPolymerTracking>. Revision 360 was the code base used to generate the results shown. The following section provides implementation specific details of the code base used to simulate the energy deposition in thin films. It is organized according to the three base classes that a user must implement in GEANT4, namely `G4VUserDetectorConstruction`, `G4VUserPhysicsList`, and `G4VUserPrimaryGeneratorAction`.

1) *Detector Geometry*: A detector geometry in GEANT4 is made up of a number of volumes. The largest volume is the `world` volume which contains all other volumes in the detector geometry. Each volume (an instance of `G4VPhysicalVolume`) is created by assigning a position, a pointer to the mother volume and a pointer to its mother volume (or `NULL` if it is the `world` volume). A volume's shape is described by `G4VSolid`, which has a shape and the specific values for each dimension. A volume's full properties is described by a logical volume. A `G4LogicalVolume` includes a pointer to the geometrical properties of the volume (the solid) along with physical characteristics including:

- the material of the volume,
- sensitive detectors of the volume and,
- any magnetic fields.

Listing 2 provides the implementation of the world physical volume. The geometry was set up such that it is possible to define multiple layers of detectors, as shown in Figure 6.

Listing 2: World Physical Volume

```
// World
```

<sup>2</sup>It should be noted that this example uses the CMAKE build system (as per the GEANT4 recommendation) but a large majority of the examples still use GNUMake for building. This can be accomplished by adding `source /opt/geant4/geant4-9.5p1/share/Geant4-9.5.1/geant4make/geant4make.sh` to the user's `.bashrc`.

```

198 2    worldS = new G4Box("World",worldSizeXY, worldSizeXY, worldSizeZ*0.5);
199    worldLV = new G4LogicalVolume(worldS,defaultMaterial,"World");
200 4    worldPV = new G4PVPlacement(0,G4ThreeVector(),worldLV,"World",0,false,0,fCheckOverlaps);
201

```

202 The detector was described by creating creating a single layer of neutron absorber and gap material and placing it  
 203 in another volume (the calorimeter). The containing volume (calorimeter) was placed inside of the the physical  
 204 world (Listing 3).

Listing 3: Calorimeter Volume

```

205    // Calorimeter (gap material)
206
207 2    caloS = new G4Tubs("Calorimeter",iRadius,oRadius,caloThickness/2,startAngle,spanAngle);
208    caloLV = new G4LogicalVolume(caloS,gapMaterial,"Calorimeter");
209 4    caloPV = new G4PVPlacement(0,G4ThreeVector(),caloLV,"Calorimeter",worldLV,false,0,
210    fCheckOverlaps);
211

```

212 The calorimeter was the mother volume for each layer. The code was developed such that the simulation of  
 213 multiple layers can be easily set at compile time or by utilizing a run macro through the DetectorMessenger  
 214 class. Multiple repeated volume can be achieved in GEANT4 through G4PVReplica or G4PVParameterised.  
 215 As each of the layers had the same geometry, G4PVReplica was chosen as the implementation (Listing 4).

Listing 4: Layer Volume

```

216    // Layer (Consists of Absorber and Gap)
217 1
218    layerS = new G4Tubs("Layer",iRadius,oRadius,layerThickness/2,startAngle,spanAngle);
219 3    layerLV = new G4LogicalVolume(layerS,defaultMaterial,"Layer");
220    if (nofLayers > 1){
221 5        layerPV = new G4PVReplica("Layer",layerLV,caloLV,kZAxis,nofLayers,layerThickness,-
222        caloThickness/2);
223    }else{
224 7        layerPV = new G4PVPlacement(0,G4ThreeVector(0.0,0.0,0.0),layerLV,"Layer",caloLV,false,0,
225        fCheckOverlaps);
226    }
227

```

228 Finally, the neutron absorber and gap material were defined as single cylinders which were then placed in the  
 229 layer mother volume (Listing 5). The size of these solids (and the materials) could be set either at compile time  
 230 through DetectorConstruction constructor or by using the DetectorMessenger in the run macro. Figure  
 231 6 shows a rendering of the 10 layers of the detector with the trajectories from a gamma event.

Listing 5: Absorber and Gap Volumes

```

232    // Absorber
233
234 2    absS = new G4Tubs("Abso",iRadius,oRadius,absThickness/2,startAngle,spanAngle);
235    absLV = new G4LogicalVolume(absS,absMaterial,"Absorber",0);
236 4    absPV = new G4PVPlacement(0,G4ThreeVector(0.0,0.0,-gapThickness/2),absLV,"Absorber",layerLV,
237    false,0,fCheckOverlaps);
238
239 6    // Gap

```

```

240 gapS = new G4Tubs("Gap", iRadius, oRadius, gapThickness/2, startAngle, spanAngle);
241 gapLV = new G4LogicalVolume(gapS, gapMaterial, "Gap", 0);
242 gapPV = new G4PVPlacement(0, G4ThreeVector(0.0, 0.0, absThickness/2), gapLV, "Gap", layerLV, false
243 , 0, fCheckOverlaps);
244

```

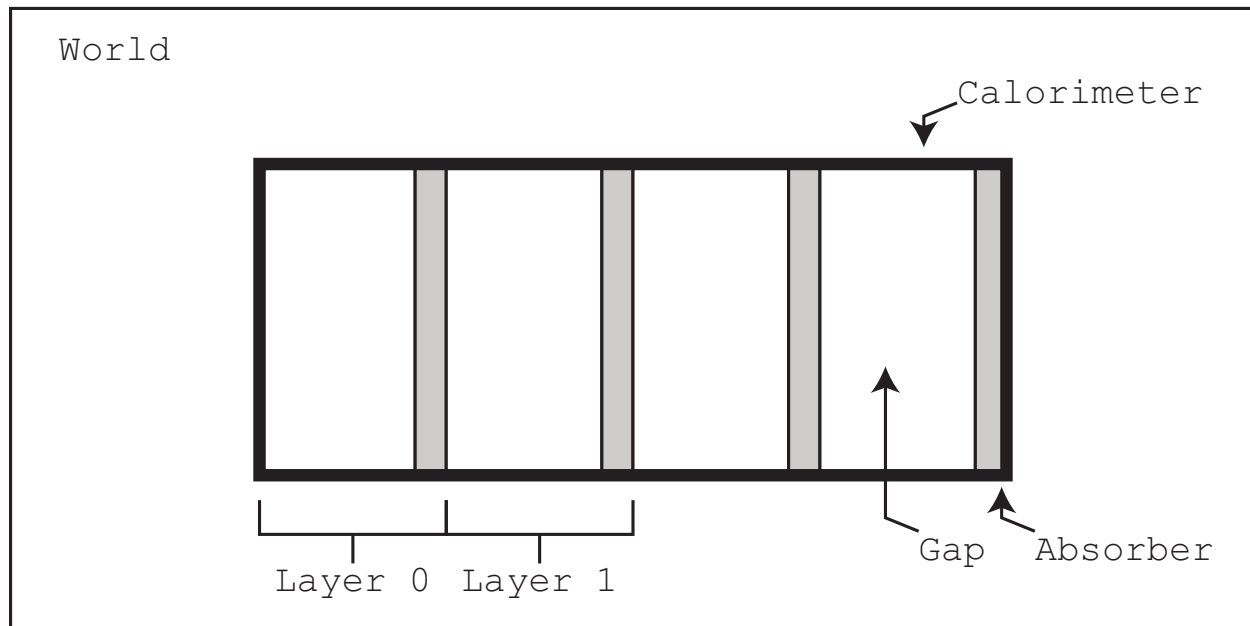


Fig. 5: World, Calorimeter, Layer and Absorber and Gap

2) *Physics Lists*: The user of the GEANT4 toolkit is responsible for selecting the proper physics processes to model in the `PhysicsList`. This is unlike other transport codes (such as MCNPX) where basic physics are enabled by default and the user only has select the appropriate cards. However, GEANT4 does provide examples of implemented `PhysicsLists` as well as modular physics lists which provide a way to construct a physics list by combining physics list. Thus, extensive use of `G4ModularPhysicsList` was employed to handle the assigning of the physics processes to each particle in the correct order. The physics lists chosen for this simulation are listed below:

- `G4EmStandardPhysics` The electromagnetic physics defines the electrons, muons, and taus along with their corresponding neutrinos. For electrons, the primary concern of this simulation, multiple scattering, electron ionization, and electron bremsstrahlung processes were assigned. In addition the positron is defined and the multiple scattering process, electron ionization process, electron bremsstrahlung process and positron annihilation is assigned [5].
- `G4EmLivermorePhysics` The Livermore physics process extend the `EMStandardPhysics` down to low (250 eV) energies. Even lower energies can be reached by including `G4DNAPhysics`. The physics processes extended with `G4EmLivermorePhysics` are the photo-electric effect, Compton scattering, Rayleigh scattering, gamma conversion, Ionisation and Bremsstrahlung[5].

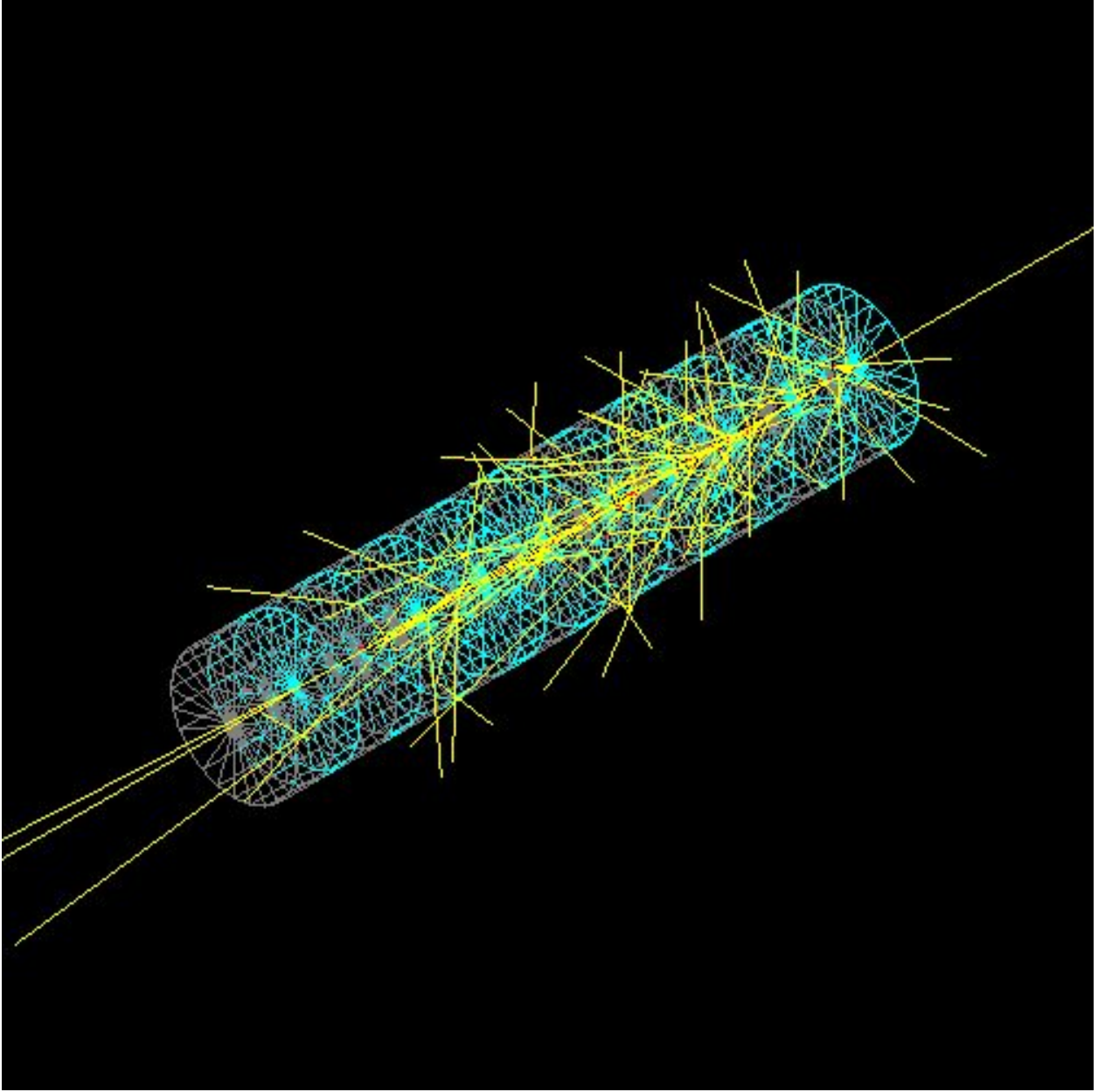


Fig. 6: 10 Layer Detector with a simulated gamma event

- `HadronPhysicsQGSP_BERT_HP` Hadronic physics are included to model the nuclear interactions. The chosen list is a Quark Gluon String Model for energies in the 5-25 GeV range, with a Bertini cascade model until 20 MeV. Once a hadron has an energy of 20 MeV the high precision cross section driven models are applied[6].
- `G4IonPhysics` Finally, to handle the transport of the charged ions resulting from an  ${}^6\text{Li}(n, \alpha){}^3\text{H}$  interaction the `G4IonPhysics` list was used.

Listing 6: Implemented Physics List

```

267
268 1 /**
269     * PhysicsList
270 3     *
271     * Constructs the physics of the simulation
272 5     */
273 PhysicsList::PhysicsList() : G4VModularPhysicsList() {
274 7     currentDefaultCut    = 10*nm;
275
276 9     // Adding Physics List
277     //RegisterPhysics( new G4EmDNAPhysics());
278 11    RegisterPhysics( new G4EmStandardPhysics());
279     RegisterPhysics( new G4EmLivermorePhysics());
280 13    RegisterPhysics( new HadronPhysicsQGSP_BERT_HP());
281     RegisterPhysics( new G4IonPhysics());
282 15 }
283

```

284 Finally, the default cut range was decreased from 1 cm to 1 nm in SetCuts() (Listing 7)

Listing 7: Implemented Physics List

```

285
286 1 void PhysicsList::SetCuts() {
287     SetDefaultCutValue(10*nm);
288 3 }
289

```

290 3) *Primary Event Generator*: The user is responsible for telling the simulation toolkit the primary event to  
291 generate. While there is great flexibility to generate any source distribution, a particle gun was chosen for simplicity.  
292 G4ParticleGun generates primary particle(s) with a given momentum and position without any randomization.  
293 The implementation of this is shown in Listing 8.

Listing 8: Primary Event Generator

```

294
295 PrimaryGeneratorAction::PrimaryGeneratorAction() : G4VUserPrimaryGeneratorAction(), fParticleGun
296     (0) {
297 2     G4int nofParticles = 1;
298     fParticleGun = new G4ParticleGun(nofParticles);
299 4
300     // default particle kinematic
301 6     G4ParticleDefinition* particleDefinition = G4ParticleTable::GetParticleTable()->FindParticle("e
302         -");
303     fParticleGun->SetParticlePosition(G4ThreeVector(0.,0.,0.0));
304 8     fParticleGun->SetParticleDefinition(particleDefinition);
305     fParticleGun->SetParticleMomentumDirection(G4ThreeVector(0.,0.,1.));
306 10    fParticleGun->SetParticleEnergy(50.*MeV);
307 }
308

```

309 Actual primary particles are generated with GeneratePrimaries, which uses the G4ParticleGun to determine  
310 the vertex of the primary event.



Listing 9: Generate Primaries

```

311
312 void PrimaryGeneratorAction::GeneratePrimaries(G4Event* anEvent)
313 {
314     // This function is called at the begining of event
315
316     // In order to avoid dependence of PrimaryGeneratorAction
317     // on DetectorConstruction class we get world volume
318     // from G4LogicalVolumeStore
319     G4double worldZHalfLength = 0;
320     G4LogicalVolume* worlLV = G4LogicalVolumeStore::GetInstance()->GetVolume("World");
321     G4Box* worldBox = 0;
322     if ( worlLV) worldBox = dynamic_cast< G4Box*>(worlLV->GetSolid());
323     if ( worldBox ) {
324         worldZHalfLength = worldBox->GetZHalfLength();
325     }
326     else {
327         G4cerr << "World volume of box not found." << G4endl;
328         G4cerr << "Perhaps you have changed geometry." << G4endl;
329         G4cerr << "The gun will be place in the center." << G4endl;
330     }
331
332     // Set gun position
333     fParticleGun->SetParticlePosition(G4ThreeVector(0., 0., -worldZHalfLength+1*cm));
334     fParticleGun->GeneratePrimaryVertex(anEvent);
335 }
336

```

### B. Sensitive Detectors and Hits

GEANT4 offers a myriad of different ways to output the results of a simulation. It is possible to write out every track with the `Verbose = 1` option, create `MultiFunctionalDetector` and `G4VPrimitiveScorer`, or implement a hit and readout based approach [7]. Previous GEANT4 experience included `G4VHit` and `G4VSensitiveDetector`, so this approach was used in this simulation. A hit is defined to be a snapshot of the physical interaction of a track in a sensitive region of a detector. As the user is responsible for implementing `G4VHit` the hit can contain any information about the step, including:

- the position and time of the step,
- the momentum and energy of the track,
- the energy deposition of the step,
- or information about the geometry.

For this simulation any information about the particle that could be recorded was recorded. This included the energy deposition, position of the hit, momentum, kinetic energy, track ID, parent ID, particle definition, volume and copy number (Listing 10).

Listing 10: Calorimeter Hit

```

351
352  /**
353  * @brief - Hit: a snapshot of the physical interaction of a track in the sensitive region of a
354  * detector
355  *
356  * Contains:
357  * - Particle Information (type and rank (primary, secondary, tertiary ...))
358  * - Position and time
359  * - momentum and kinetic energy
360  * - deposition in volume
361  * - geometric information
362  */
363 class CaloHit : public G4VHit {
364 public:
365     CaloHit(const G4int layer);
366     ~CaloHit();
367
368     inline void* operator new(size_t);
369     inline void operator delete(void*);
370     void Print();
371
372 private:
373     G4double edep;           /* Energy Deposited at the Hit */
374     G4ThreeVector pos;       /* Position of the hit */
375     G4double stepLength;     /* Step Length */
376     G4ThreeVector momentum;  /* Momentum of the step */
377     G4double kEnergy;        /* Kinetic Energy of the particle */
378     G4int trackID;           /* Track ID */
379     G4int parentID;          /* Parent ID */
380     G4ParticleDefinition* particle; /* Particle Definition */
381     G4int particleRank;       /* Primary, Secondary, etc */
382     G4VPhysicalVolume* volume; /* Physical Volume */
383     G4int layerNumber;        /* Copy Number of Layer */
384
385 public:
386     // Setter and Getters
387 };
388
389 typedef G4THitsCollection<CaloHit> CaloHitsCollection;
390 extern G4Allocator<CaloHit> HitAllocator;
391
392 inline void* CaloHit::operator new(size_t){
393     void *aHit;
394     aHit = (void *) HitAllocator.MallocSingle();
395     return aHit;
396 }
397
398 inline void CaloHit::operator delete(void *aHit){

```

```

399 HitAllocator.FreeSingle((CaloHit*) aHit);
400 }
401

```

402 The G4VSensitiveDetector is attached to a logical volume and is responsible for filling the hit collection.  
 403 This is accomplished in ProcessHits of CaloSensitiveDetector (Listing 11).

Listing 11: Sensitive Detector

```

404 /**
405  * ProcessHits
406  *
407  *
408  * Adds a hit to the sensitive detector, depending on the step
409  */
410 G4bool CaloSensitiveDetector::ProcessHits(G4Step* aStep,G4TouchableHistory*) {
411
412     G4double edep = aStep->GetTotalEnergyDeposit();
413     G4double stepLength = aStep->GetStepLength();
414
415     // Getting the copy number
416     G4TouchableHistory* touchable = (G4TouchableHistory*)
417         (aStep->GetPreStepPoint()->GetTouchable());
418     G4int layerIndex = touchable->GetReplicaNumber(1);
419
420     // Creating the hit
421     CaloHit* newHit = new CaloHit(layerIndex);
422     newHit->SetTrackID(aStep->GetTrack()->GetTrackID());
423     newHit->SetParentID(aStep->GetTrack()->GetParentID());
424     newHit->SetEdep(edep);
425     newHit->SetStepLength(stepLength);
426     newHit->SetPosition(aStep->GetPreStepPoint()->GetPosition());
427     newHit->SetLayerNumber(layerIndex);
428     newHit->SetMomentum(aStep->GetPreStepPoint()->GetMomentum());
429     newHit->SetKineticEnergy(aStep->GetPreStepPoint()->GetKineticEnergy());
430     newHit->SetParticle(aStep->GetTrack()->GetDefinition());
431     newHit->SetVolume(aStep->GetTrack()->GetVolume());
432
433     // Adding the hit to the collection
434     hitCollection->insert( newHit );
435
436     return true;
437 }
438

```

439 The simulation was designed so that a separate sensitive detector was assigned to the gap and absorber. While this is  
 440 not strictly necessary as the geometric position determines what layer of the gap or absorber the hit occurred in, this  
 441 made the analysis code easier to write. A separate method was written in DetectorConstruction to create  
 442 the sensitive detectors and assign them to the proper logical volumes (Listing 12) SetSensitiveDetectors()  
 443 is called from the the constructor of DetectorConstruction.

Listing 12: Creating Sensitive Detectors

```

444
445 1 /**
446     * SetSensitiveDetectors
447 3     *
448     * Setting the Sensitive Detectors of the Detector
449 5     */
450 void DetectorConstruction::SetSensitiveDetectors() {
451 7     G4SDManager* SDman = G4SDManager::GetSDMpointer();
452     absSD = new CaloSensitiveDetector("SD/AbsSD", "AbsHitCollection");
453 9     SDman->AddNewDetector(absSD);
454     absLV->SetSensitiveDetector(absSD);
455 11
456     gapSD = new CaloSensitiveDetector("SD/GapSD", "GapHitCollection");
457 13     SDman->AddNewDetector(gapSD);
458     gapLV->SetSensitiveDetector(gapSD);
459 15 }
460

```

### 461 C. Analysis

462 Analysis of hit collection was preformed with ROOT. Once again there are other options (notably OpenScientist)

463 but previous experience was why ROOT was selected as the base for the Analysis framework. A singleton class

464 was written for the analysis which processed the hit collections, assigning the various results to root histograms.

465 User action classes EventAction and RunAction are called at the beginning and end of each run and event,

466 respectively (Listing 13,14). These classes allowed for the analysis code to be independent of the simulation.

Listing 13: Event Action

```

467
468 1 EventAction::EventAction() : G4UserEventAction() {
469     // Nothing to be Done Here
470 3 }
471
472 5 /**
473     * BeginOfEventAction
474 7     *
475     * @param const G4Event* event - event to be processed
476 9     *
477     * At the begining of an event we want to clear all the event
478 11     * accumulation variables.
479     */
480 13 void EventAction::BeginOfEventAction(const G4Event* event) {
481     Analysis::GetInstance()->PrepareNewEvent(event);
482 15 }
483
484 17 /**
485     * EndOfEventAction
486 19     *
487     * @param const G4Event* event - event to be processed

```

```

48821 *
489 * At the end of an event we want to call analysis to process
49023 * this event, and record the useful information.
491 */
49225 void EventAction::EndOfEventAction(const G4Event* event) {
493     Analysis::GetInstance()->EndOfEvent(event);
49427 }
495

```

Listing 14: Run Action

```

496
4971 RunAction::RunAction() : G4UserRunAction() { }
498
4993 void RunAction::BeginOfRunAction(const G4Run* run) {
500     G4cout<<"Starting run: " << run->GetRunID()<< G4endl;
5015     Analysis::GetInstance()->PrepareNewRun(run);
502 }
5037
504 void RunAction::EndOfRunAction(const G4Run* aRun) {
5059     Analysis::GetInstance()->EndOfRun(aRun);
506 }
507

```

#### 508 D. Determination of Energy Deposition

The energy deposition of an event is calculated by the sum of all of the energy deposited by individual hits in the sensitive detector (Equation 1). While it is possible to break down the energy deposition by which physics process caused the deposition, this was not implemented in order to avoid over complication.

$$E_{\text{dep,event}} = \sum E_{\text{dep,hit}} \quad (1)$$

509 ProcessHitCollection is called at the end of each event (Listing 15). Each hit is accessed and the layer at  
 510 which it occurs is determined<sup>3</sup>. In addition the name of the volume is determined, and the energy deposition of the  
 511 hit is added to the energy deposition of the event. If the hit occurred in the `absorber` layer and the particle is an  
 512 electron the kinetic energy of that hit is also recorded.

Listing 15: Process Hit Collection

```

513
5141 /**
515 * ProcessHitCollection
5163 *
517 * @param G4VHitsCollection *hc
5185 */
519 void Analysis::ProcessHitCollection(G4VHitsCollection *hc,G4int eventID){
5207
521     // Looping through the hit collection

```

<sup>3</sup>C arrays start at 0, so memory is allocated for one more than the total number of layers. This allows for `NUMLAYERS+1` to be used as an index into the histogram for the total of all layers in the material (either gap or absorber).

```

522 9      G4double hitColEdepTot_Abs[NUMLAYERS+1];    // Total EDep (abs) for Hit Collection
523      G4double hitColEdepTot_Gap[NUMLAYERS+1];    // Total EDep (gap) for Hit Collection
524 11      G4int PID;                                // Parent ID
525      for(int i= 0; i < NUMLAYERS+1; i++){
526 13          hitColEdepTot_Abs[i] = 0.0;
527          hitColEdepTot_Gap[i] = 0.0;
528 15      }
529
530 17      // Energy Deposition of the event
531      for(G4int i = 0; i < hc->GetSize(); i++){
532 19          CaloHit* hit = (CaloHit*) hc->GetHit(i);
533
534 21          G4double eDep = hit->GetEdep();
535          G4int layerNum = hit->GetLayerNumber();
536 23          if (strcmp(hit->GetVolume()->GetName(),"Gap")){
537              // Hit occurred in the Gap
538 25              hitColEdepTot_Gap[layerNum] += eDep;
539              (hHitTotEdepGap[layerNum])->Fill(eDep);
540 27          }else if (strcmp(hit->GetVolume()->GetName(),"Absorber")){
541              // Hit occurred in the Abs
542 29              hitColEdepTot_Abs[layerNum] += eDep;
543              (hHitTotEdepAbs[layerNum])->Fill(eDep);
544 31
545              /* Is this a secondary electron of the event? */
546 33              if(hit->GetParticle()->GetPDGEncoding() == 11){
547                  PID = hit->GetParentID();
548 35                  if (PID < NUMPID){
549                      (hSecElecKinAbs[layerNum][PID])->Fill(hit->GetKineticEnergy());
550 37                  }
551              }
552 39          }
553          else{
554 41              G4cout<<"ERROR - Unkown Volume for sensitive detector"<<G4endl;
555          }
556 43      }
557
558 45      // Adding this Hit collection's energy deposited to event total
559      for (int i = 0; i < NUMLAYERS; i++){
560 47          // Incrementing each individual bin
561          eventEdepTot_Abs[i] += hitColEdepTot_Abs[i];
562 49          eventEdepTot_Gap[i] += hitColEdepTot_Gap[i];
563
564 51          // Last bin is Calorimter Total (all Abs layers and all Gap layers)
565          eventEdepTot_Abs[NUMLAYERS] += hitColEdepTot_Abs[i];
566 53          eventEdepTot_Gap[NUMLAYERS] += hitColEdepTot_Gap[i];
567      }
568 55  }
569

```

Finally, a run macro was written to control the entire run (Listing 16). The material and thickness of the detector are declared (made possible by the use of `DetectorMessenger`), and then the detector is dynamically updated. A  $^{60}\text{Co}$  source is simulated by shooting photons of the 1.1732 MeV and 1.3325 MeV. The source particle is then changed to a neutron, and thermal (0.025 eV) neutrons are shot at the detector. The thickness of the absorber is then increased, the geometry updated, and the entire process repeated. As these runs tend to take a large amount of time, GEANT4 was parallelized for use with MPI to take advantage of the cluster computing power.

Listing 16: Run Macro

```

576 #
577 /tracking/verbose 0
578 #
579 # Setting up the detector
580 #
581 /PolymerTransport/det/setAbsMat PS_Detector
582 /PolymerTransport/det/setGapMat G4_POLYSTYRENE
583 /PolymerTransport/det/setGapThick 0.3175 cm
584 #
585 /PolymerTransport/det/setAbsThick 15 um
586 /PolymerTransport/det/update
587 # Cobalt 60
588 /gun/particle gamma
589 /gun/direction 0 0 1
590 /gun/energy 1.1732 MeV
591 /run/beamOn 500000000 # 500 Million
592 /gun/energy 1.3325 MeV
593 /run/beamOn 500000000 # 500 Million
594 # Neutron
595 /gun/particle neutron
596 /gun/energy 0.025 eV
597 /run/beamOn 1000000 # 1 Million
598 #
599 /PolymerTransport/det/setAbsThick 25 um
600 /PolymerTransport/det/update
601
602

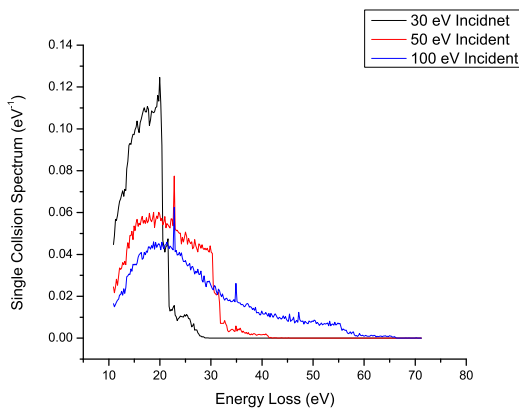
```

#### IV. SIMULATION VALIDATION

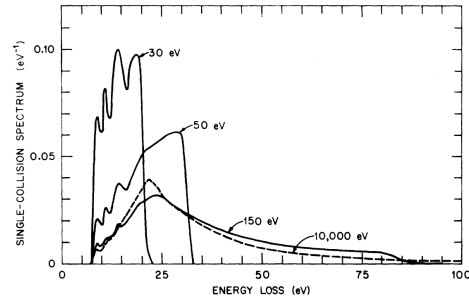
GEANT4 is a toolkit implemented by the user so extensive efforts were completed in order to validate the results and ensure no bugs exists. First steps were taken (for small runs) to compute the energy deposition for small runs by hand in order to make sure they agreed with the analysis code. In addition the reaction products of the  ${}^6\text{Li}(n, \alpha){}^3\text{H}$  were checked to make sure that they agreed with the published values<sup>4</sup>. The GEANT4 simulation was validated by comparing the single collision energy loss spectra in water and by comparing the simulation energy deposition to that of a measured spectra.

##### A. Energy Deposition Validation

The energy deposition was tested by reproducing the single collision energy loss spectra in water<sup>5</sup>. The PhysicsList was extended to include G4DNAPhysics and the detector material was set to the NIST definition contained in the toolkit with `G4Material* H2O = man->FindOrBuildMaterial("G4_WATER")`. In general there was excellent agreement between the simulated energy spectra and a previously published spectra[1]. The simulated spectra had much better resolution at fine energies (corresponding to discrete states) of which Turners did not.



(a) Simulated



(b) Single-collision energy loss spectra for electrons in water [1]

(c) Published

Fig. 7: Single Collision Energy Loss of Water

<sup>4</sup>GEANT4 4.9.2.p01 contains an error in which extra photons are generated, This has been fixed in the release used, 4.9.5p1

<sup>5</sup>An analysis class was not written for this simulation. Instead the verbosity of the simulation was set to `verbose=1` in the run macro. The first ionisation collision (`e-_G4DNAIonisation`) was then extracted with `sed -n '/ParentID = 0/,/e-_G4DNAIonisation/p' G4OutputFileName.txt | grep "e-_G4DNAIonisation" | awk '{print $5}'`



## 617 *B. Spectra Validation*

The simulated energy deposition is not the directly equivalent to light collected on the PMT because the scintillation process and light collection is not modeled. However, it is well known that scintillation follows the energy deposition[8]. Thus, up to scaling constants, the energy deposition can be considered equivalent to the scintillation and representative of the measured spectra. Rather than attempting to back out these scaling constants the weighted average of spectra were used in which integration and normalization removes these fudge factors. The simulation was validated by computing the weighted average of the energy deposition 2 and comparing it to the spectra average defined in 3. There is excellent agreement between the measured gamma weighted average (right ordinate axis) and the average energy deposition from a  $^{60}\text{Co}$  source (left ordinate axis). Non-linearity is observed for films less than 200  $\mu\text{m}$ , this is evidence that the cascade electrons from the Compton electron are energetic enough that the range of the electrons is much greater than the thickness of the film and leave the film without colliding to an energy in which the energy deposition is linear (Figure 4).

$$\langle E \rangle = \frac{\int_0^\infty \phi(E) E dE}{\int_0^\infty \phi(E) dE} \text{ where} \quad (2)$$

$$\langle \mu \rangle = \frac{\int_0^\infty f(x) x dx}{\int_0^\infty f(x) dx} \text{ where} \quad (3)$$

618

The comparison between the average energy deposition and measured channel allows for the a relationship to be drawn between the energy deposited and the channel number. This is completed by an taking an average of the ratio between the average channel number (Equation 3 and the average energy deposition (Equation 2). This ratio is defined in Equation 4. This quantity is defined separately for neutrons and gammas.

$$\eta = \sum_t \frac{\langle E \rangle}{\langle \mu \rangle} \quad (4)$$

Fig. 8: Gamma Simulation Agreement

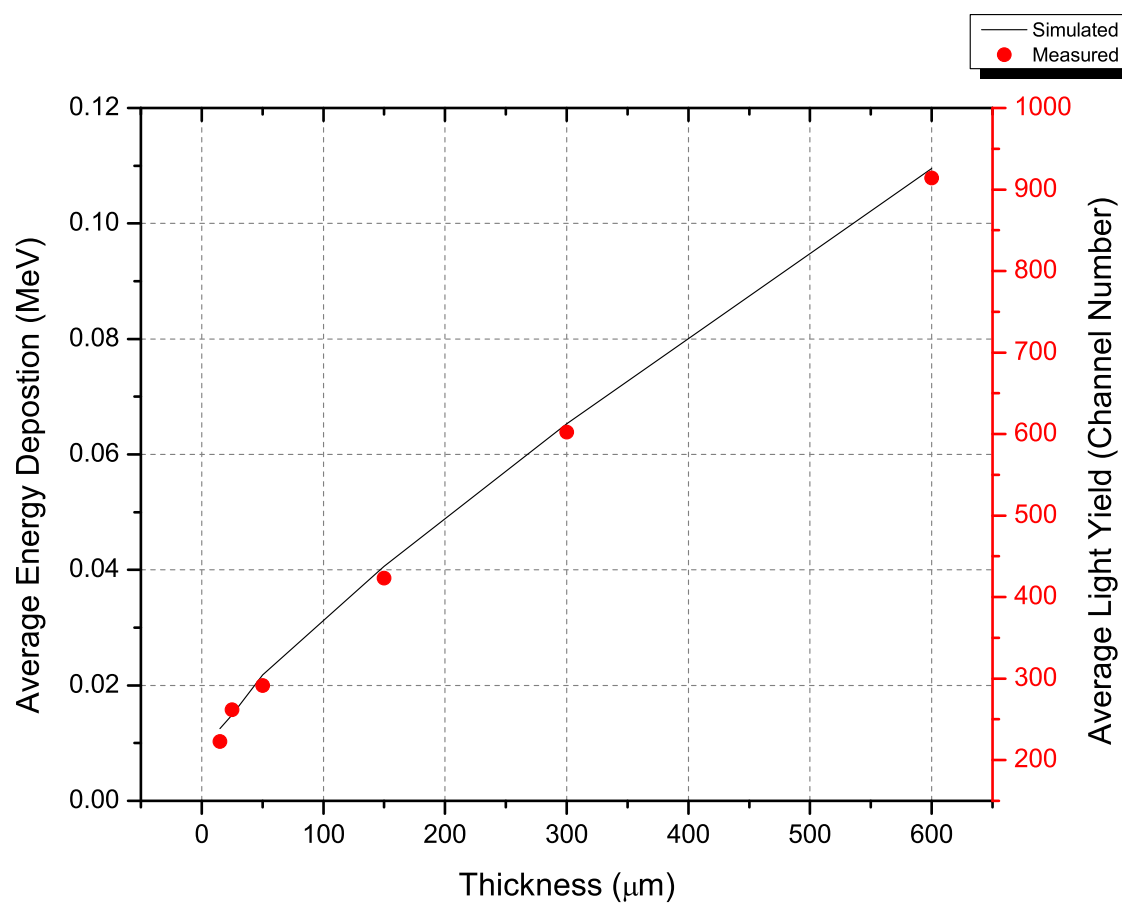
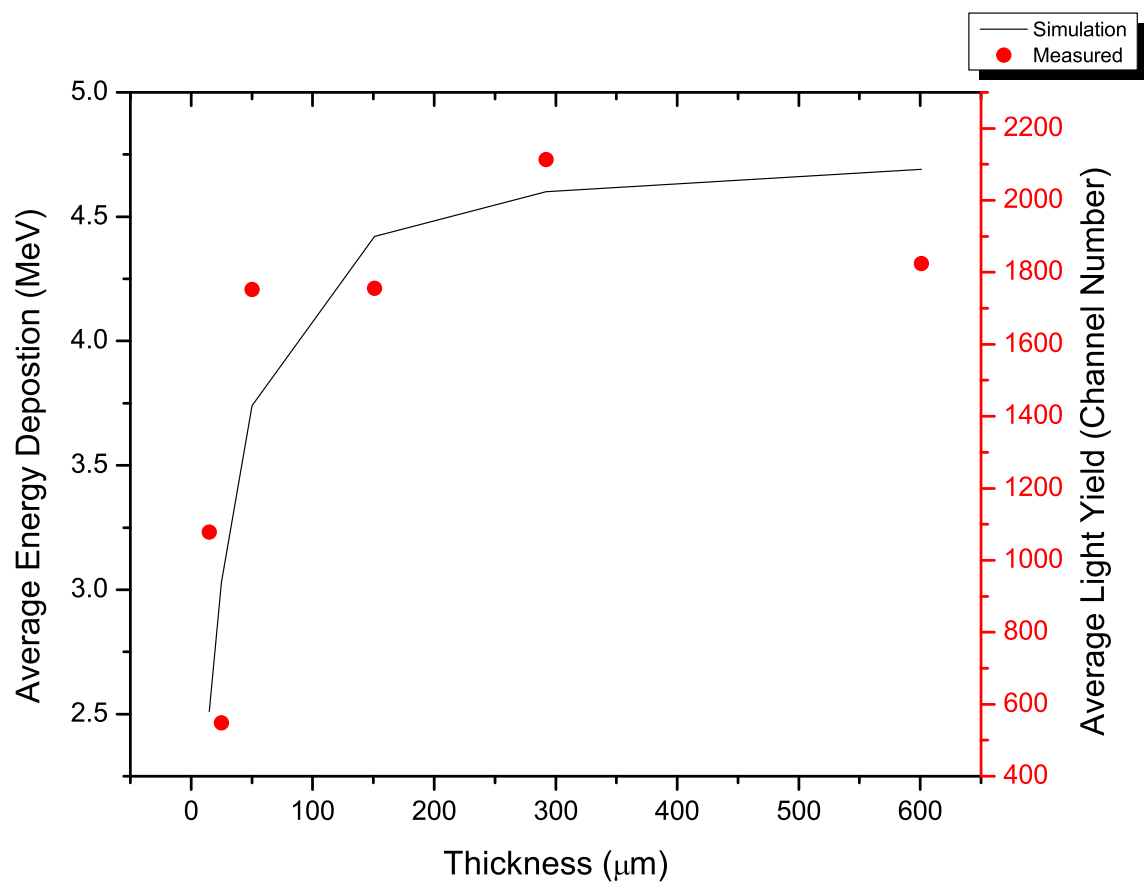


Fig. 9: Neutron Simulation Agreement



## V. RESULTS

### A. Energy Deposition

The energy deposition was calculated for neutron and gamma events for films of thickness of 15  $\mu\text{m}$ , 25  $\mu\text{m}$ , 50  $\mu\text{m}$ , 150  $\mu\text{m}$ , 300  $\mu\text{m}$ , 600  $\mu\text{m}$ , 1 mm and 1 cm (Figure 10, 11).

Photons have a very low probability of interacting in the film due to polymer film being a low  $z$ -material. This is reflected in the majority of the events not interacting at all; about 1 in 10,000 of the events deposit energy in the film as seen in Figure 10. Several classic features of the spectra are apparent on the 1 cm thick film. These included the photo-peak in which all of the incident energy of the  $^{60}\text{Co}$  is deposited in the film, as well as the individual Compton edges of the two photons from  $^{60}\text{Co}$ . These features are not visible on the measured spectra due to the poor energy resolution of these films. There is also physical evidence of a lack of a Compton edge on the thinner films, but the films greater than 150  $\mu\text{m}$  thick show some feature around 0.2 MeV. Films thinner than 150  $\mu\text{m}$  show a very small amount of energy deposition that quickly tails off for higher energies, indicating that when a photon interaction occurs in the film the electrons from that interaction leave the film and the only energy deposition occurs from small ionizations as the highly energetic electron leaves the film material. It is also observed that the thinnest film (15  $\mu\text{m}$ ) has an average energy deposition of around 10 keV, while the 1 cm film has an average energy deposition of around 150 keV. The simulated energy deposition for neutron interactions in thin films is shown in Figure 11. Several features of the spectra can be immediately noted. For thick films (1 cm) there is a very high probability that a given event will deposit all of its energy in the film (as expected). Thinner films have a smaller probability of depositing all of their energy, but this is overshadowed by the thick samples when plotted. It is also interesting to note that it is possible to observe the comparative effects of the  $\alpha$  and  $^3\text{H}$  in the neutron energy deposition spectra. The triton has a much shorter range ( $\sim 10 \mu\text{m}$  in PS [9]) than the  $\alpha$  ( $\sim 60 \mu\text{m}$ ) so it has a higher probability of depositing all of its energy. Thus, for energies above 2.73 MeV (the energy of the triton) there is a higher probability of energy deposition (by about a factor of 10). These events are still very infrequent compared to the probability of depositing all of the reaction product energy. Even for the 15  $\mu\text{m}$  the average energy deposition was above 50% of the total  $Q$ -value of the reaction, and by 200  $\mu\text{m}$  this average energy deposited approaches 95% of the total 4.78 MeV.

### B. Secondary Electron Energy Distribution

The distribution of secondary electrons from photon interactions are plotted in Figure 12. From these results it can be concluded that it is unlikely (around 1 in 10,000) that an electron will be scattered with the maximum Compton scattering kinetic energy, but rather have an energy somewhat lower than that. The distribution of secondary electrons from photon interactions is actually very flat, implying that it is likely for the electron from a Compton scattering event to have an energy in the 100's of keV. The distribution of the next generation of electrons was also calculated, and this distribution was also quite energetic (with a maximum energy corresponding to 0.55 MeV) but with a much large probability of having a collision that produces an electron with a much lower energy.

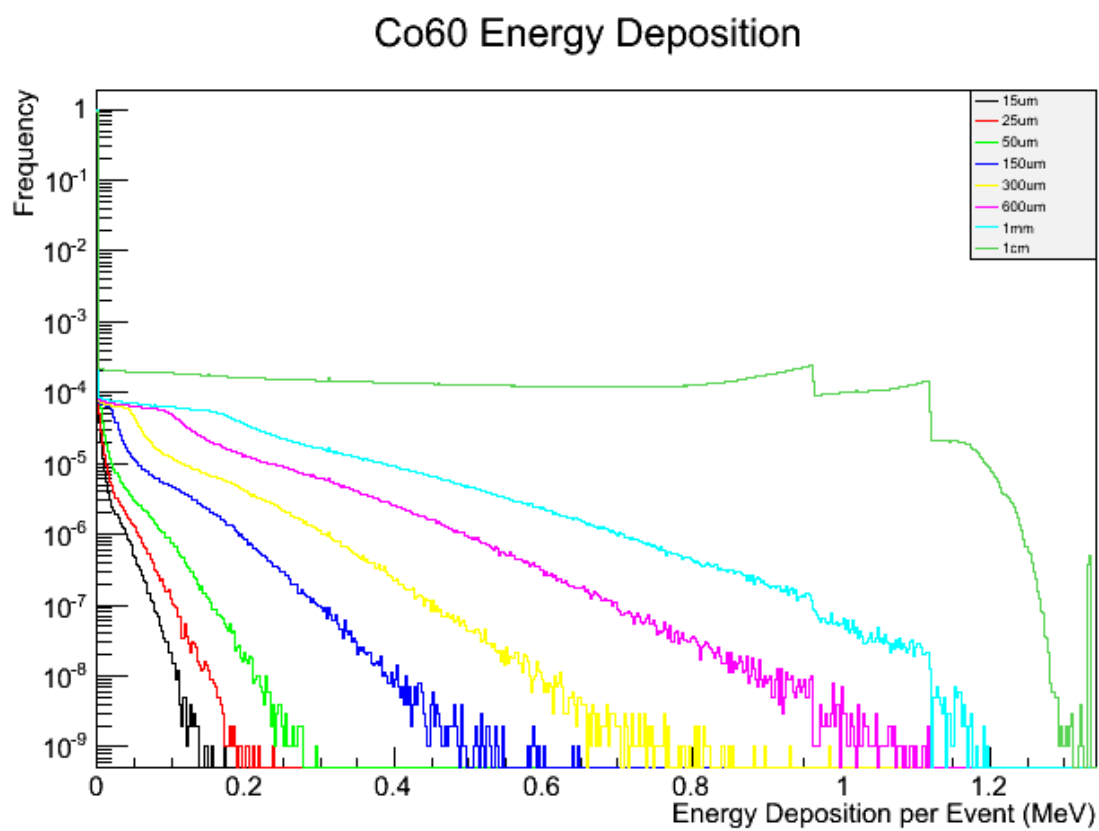


Fig. 10: Simulated Energy Deposition for a Single Film (gammas)

## Energy Deposition

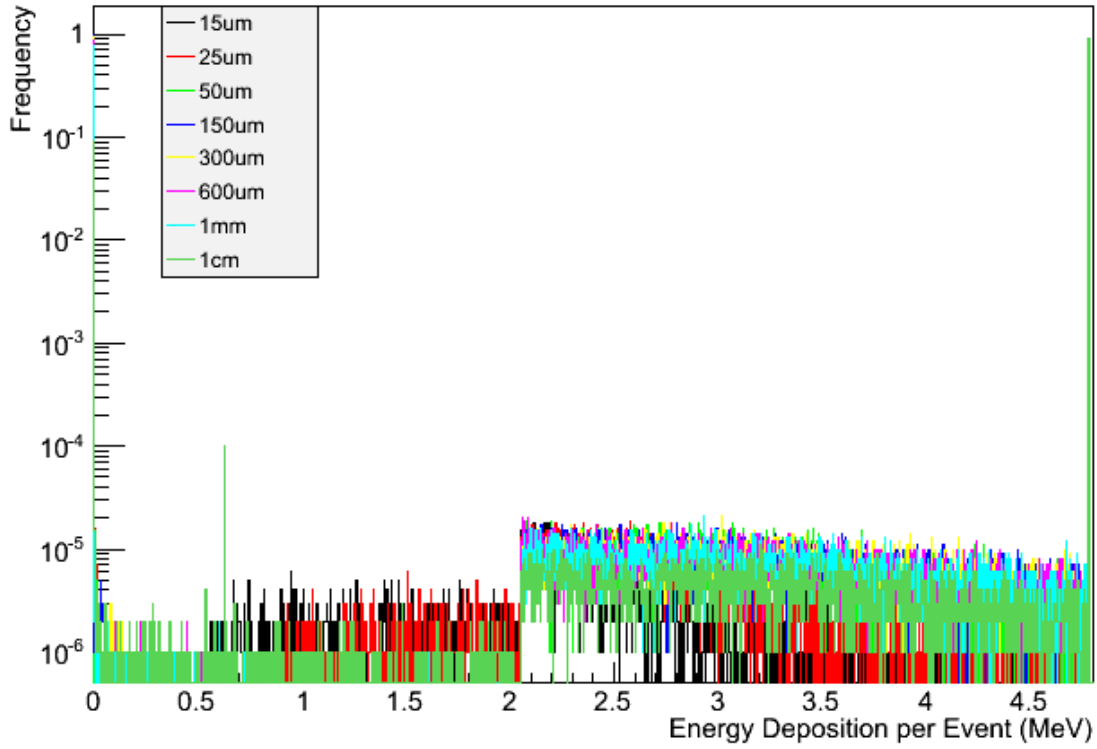


Fig. 11: Simulated Energy Deposition for a Single Film (neutrons)

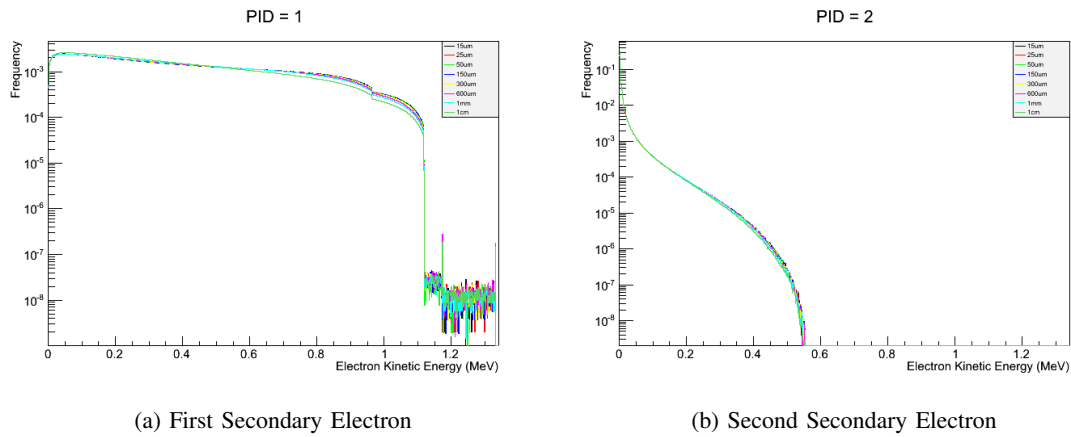


Fig. 12: Simulated kinetic energies of electrons from  $^{60}\text{Co}$  interactions

## VI. CONCLUSIONS

GEANT4 has been employed to simulate the energy spectra of electrons and energy deposition from thermal neutrons and  $^{60}\text{Co}$  gammas. A versatile implementation of the geometry was used in which it is possible to dynamically set the materials, thickness, and number of layers between runs. In addition, analysis methods have been written to aid in the reporting of the results. This simulation was verified by reproducing the single collision energy loss spectra for water, and also by comparing the average energy deposited to the measured average channel number for film ranging from  $15\mu\text{m}$  to  $600\mu\text{m}$ .

The energy deposition of the films were calculated and plotted in Figure 11 and Figure 10. It is then observable that the gamma interactions have a very low probability of depositing a majority of the energy from a  $^{60}\text{Co}$  photon into the material, while neutrons tend to deposit over 50% of their energy in the material for a  $15\mu\text{m}$  film, and increasing to 96% for a 1 cm thick film. Figure 13 shows the average energy deposition as a function of thickness for neutrons and gammas, along with the calculated channel number (according to Equation 4). At thickness of less than  $200\mu\text{m}$  there is significant separation between the average energy deposited by neutron events compared to gamma events. As the thickness of the films increased the average neutron energy approached the asymptotic limit of 4.78 MeV, while the average gamma energy increased. This creates less separation between the two, and provides less of an ability for neutron-gamma discrimination based on pulse height.

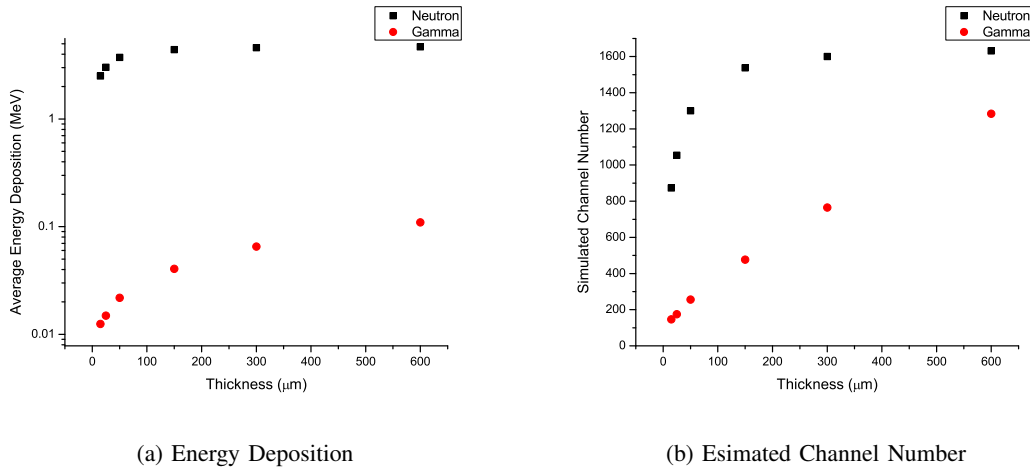


Fig. 13: Comparison between average neutron and gamma energy deposition

## REFERENCES

- [1] J. E. Turner, H. G. Paretzke, R. N. Hamm, H. A. Wright, and R. H. Ritchie, "Comparative study of electron energy deposition and yields in water in the liquid and vapor phases," *Radiation Research*, vol. 92, pp. 47–60, Oct. 1982. ArticleType: research-article / Full publication date: Oct., 1982 / Copyright 1982 Radiation Research Society.
- [2] S. Agostinelli, J. Allison, K. Amako, J. Apostolakis, H. Araujo, P. Arce, M. Asai, D. Axen, S. Banerjee, G. Barrand, F. Behner, L. Bellagamba, J. Boudreau, L. Broglia, A. Brunengo, H. Burkhardt, S. Chauvie, J. Chuma, R. Chytrcek, G. Cooperman, G. Cosmo, P. Degtyarenko, A. Dell'Acqua, G. Depaola, D. Dietrich, R. Enami, A. Feliciello, C. Ferguson, H. Fesefeldt, G. Folger, F. Foppiano, A. Forti, S. Garelli, S. Giani, R. Giannitrapani, D. Gibin, J. Gmez Cadenas, I. Gonzlez, G. Gracia Abril, G. Greeniaus, W. Greiner, V. Grichine, A. Grossheim, S. Guatelli, P. Gumplinger, R. Hamatsu, K. Hashimoto, H. Hasui, A. Heikkinen, A. Howard, V. Ivanchenko, A. Johnson, F. Jones, J. Kallenbach, N. Kanaya, M. Kawabata, Y. Kawabata, M. Kawaguti, S. Kelner, P. Kent, A. Kimura, T. Kodama, R. Kokoulin, M. Kossov, H. Kurashige, E. Lamanna, T. Lampn, V. Lara, V. Lefebvre, F. Lei, M. Liendl, W. Lockman, F. Longo, S. Magni, M. Maire, E. Medernach, K. Minamimoto, P. Mora de Freitas, Y. Morita, K. Murakami, M. Nagamatsu, R. Nartallo, P. Nieminen, T. Nishimura, K. Ohtsubo, M. Okamura, S. O'Neale, Y. Oohata, K. Paech, J. Perl, A. Pfeiffer, M. Pia, F. Ranjard, A. Rybin, S. Sadilov, E. Di Salvo, G. Santin, T. Sasaki, N. Savvas, Y. Sawada, S. Scherer, S. Sei, V. Sirotenko, D. Smith, N. Starkov, H. Stoecker, J. Sulkimo, M. Takahata, S. Tanaka, E. Tcherniaev, E. Safai Tehrani, M. Tropeano, P. Truscott, H. Uno, L. Urban, P. Urban, M. Verderi, A. Walkden, W. Wander, H. Weber, J. Wellisch, T. Wenaus, D. Williams, D. Wright, T. Yamada, H. Yoshida, and D. Zschesche, "Geant4a simulation toolkit," *Nuclear Instruments and Methods in Physics Research Section A: Accelerators, Spectrometers, Detectors and Associated Equipment*, vol. 506, pp. 250–303, July 2003.
- [3] G. Collaboration, "Geant4 user's guide for application developers." <http://geant4.web.cern.ch/geant4/UserDocumentation/UsersGuides/ForApplicationDeveloper/html/in> Dec. 2011. Version geant4 9.5.0.
- [4] J. Allison, K. Amako, J. Apostolakis, H. Araujo, P. Dubois, M. Asai, G. Barrand, R. Capra, S. Chauvie, R. Chytrcek, G. Cirrone, G. Cooperman, G. Cosmo, G. Cuttone, G. Daquino, M. Donszelmann, M. Dressel, G. Folger, F. Foppiano, J. Generowicz, V. Grichine, S. Guatelli, P. Gumplinger, A. Heikkinen, I. Hrivnacova, A. Howard, S. Incerti, V. Ivanchenko, T. Johnson, F. Jones, T. Koi, R. Kokoulin, M. Kossov, H. Kurashige, V. Lara, S. Larsson, F. Lei, O. Link, F. Longo, M. Maire, A. Mantero, B. Mascialino, I. McLaren, P. Lorenzo, K. Minamimoto, K. Murakami, P. Nieminen, L. Pandola, S. Parlati, L. Peralta, J. Perl, A. Pfeiffer, M. Pia, A. Ribon, P. Rodrigues, G. Russo, S. Sadilov, G. Santin, T. Sasaki, D. Smith, N. Starkov, S. Tanaka, E. Tcherniaev, B. Tome, A. Trindade, P. Truscott, L. Urban, M. Verderi, A. Walkden, J. Wellisch, D. Williams, D. Wright, and H. Yoshida, "Geant4 developments and applications," *Nuclear Science, IEEE Transactions on*, vol. 53, pp. 270–278, Feb. 2006.
- [5] CERN, "Physics lists EM constructors in geant4 9.3." [http://geant4.cern.ch/geant4/collaboration/working\\_groups/electromagnetic/physlist9.3.shtml](http://geant4.cern.ch/geant4/collaboration/working_groups/electromagnetic/physlist9.3.shtml), Feb. 2012.
- [6] CERN, "Reference physics lists." [http://geant4.cern.ch/support/proc\\_mod\\_catalog/physics\\_lists/referencePL.shtml](http://geant4.cern.ch/support/proc_mod_catalog/physics_lists/referencePL.shtml), Oct. 2008.
- [7] CERN, "Detector definition and response." <http://geant4.web.cern.ch/geant4/UserDocumentation/UsersGuides/ForApplicationDeveloper/html/ch04s04.html>, 2012.
- [8] J. B. Birks, "Scintillations from organic crystals: Specific fluorescence and relative response to different radiations," *Proceedings of the Physical Society. Section A*, vol. 64, pp. 874–877, Oct. 1951.
- [9] H. Kudo and K. Tanaka, "Recoil ranges of 2.73 MeV tritons and yields of  $^{18}\text{F}$  produced by the  $^{16}\text{O}(t,n)^{18}\text{F}$  reaction in neutron-irradiated lithium compounds containing oxygen," *The Journal of Chemical Physics*, vol. 72, no. 5, p. 3049, 1980.